Journal of Membrane Science & Research

journal homepage: www.msrjournal.com

Research Paper

Novel Application of Pe Self-Adhesive Wallpaper to Replace Costly Membranes in Photosynthesis Microbial Desalination Cell for Simultaneous Seawater Desalination, Sewage Treatment, and Energy Recovery

Zainab Ziad Ismail [1, *], Ahmed Mustafa Sadeq [1, 2]

[1] *Department of Environmental Engineering University of Baghdad, Baghdad, Iraq*
[2] *Ministry of Environment, Baghdad, Iraq*

Article info

Received 2025-02-20
Revised 2025-07-01
Accepted 2025-07-03
Available online 2025-07-03

Keywords

Photosynthesis microbial desalination cell
Membranes
PE foam self-adhesive wall panels
Biocathode
Desalination
Bioenergy recovery

Highlights

- Performance of membraneless-photosynthesis microbial desalination cell (PMDC) was evaluated.
- Novel application of Pe self-adhesive wallpaper material as a separator between PMDC compartments.
- Maximum desalination efficiency of actual seawater was 83% with the absence of fouling.
- Maximum COD removal efficiency from the real sewage was 99.6%.
- Maximum recorded power output in the PMDC was 489 mW/m^3.

Graphical abstract

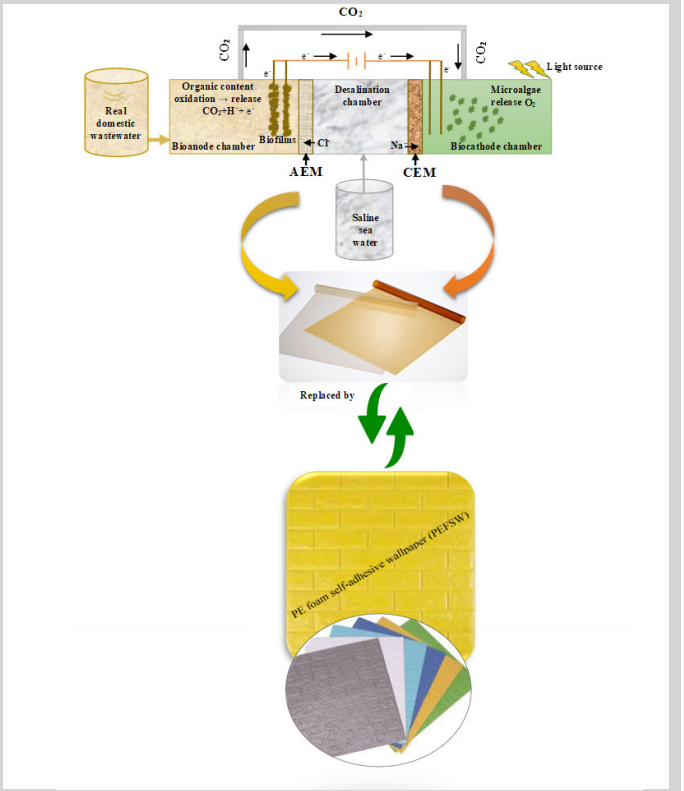

Abstract

There is a global drive to apply sustainable techniques such as photosynthetic microbial desalination cells (PMDCs) for simultaneous wastewater treatment, desalination of saline water, and power generation. However, the exorbitant expense of the typical membranes employed in PMDCs has limited their broad usage. This study attempts to overcome this challenge by investigating for the first time the potential of using inexpensive PE foam self-adhesive wall panels (PEFSW) material as a separator between the three compartments in the PMDC to replace the costly typical cation and anion exchange membranes. Two identically designed PMDCs were constructed, setup, and continually operated for 180 days. The membraneless-PMDC was equipped with PEFSW sheets, whereby, the membrane-PMDC was assembled with the conventional cation and anion exchange membranes. Both PMDCs were continually fed with real sewage into the anaerobic anode chamber and actual saline seawater into the desalination chamber. Results revealed that the membraneless-PMDC exhibited remarkable maximum desalination elimination efficiency, organic content removal efficiency, and power output of 83%, 99.6%, and 489 mW/m^3 versus 81%, 98.1%, and 430 mW/m^3, in membrane-PMDC, respectively. Also, four different growth kinetic models including Blackman, Moser, Monod, and Teissier were adopted to describe the relevance between anodic biofilm development and substrate utilization in the PMDCs. The results revealed that the four models demonstrated excellent fitting with the experimental results with determination coefficients (R^2) ranged between 0.94 to 0.96. The beauty of the suggested innovative approach is the absence of PEFSW fouling during the operation period and being inexpensive option.

* Corresponding author: dr.zainab.zead@coeng.uobaghdad.edu.iq (Z. Z. Ismail)

DOI: 10.22079/jmsr.2025.2053942.1705

1. Introduction

The increased demanding for water from several different sectors led to increasing the global water and energy consumption at a rate exceeded the growth rate of population [1]. According to a UN report, approximately 2.2 billion people lack access to safely managed drinking water services, highlighting the urgent need for sustainable water solutions. Also, the seas and oceans waters are estimated at approximately 75 % of the Earth's surface, which involve a striking water volume of nearly 1.3×10^{18} tons. Desalination process involves the salt elimination and removal from the saline water to get a potable or drinkable water. Due to the growing concerns of water security, an extensive studies and investment in desalination, resulting in rapid industrial expansion over the past 40 years [2, 3]. Although desalination of seawater by reverse osmosis and other desalination technologies including electrodialysis, multistage distillation, and capacitive deionization can provide significant production of potable water, but still there many challenges such as high-power consumption and discharge of brine [4].

In response, the search for more economical desalination technologies and alternative energy sources has led to microbial desalination cell (MDC) and photosynthesis microbial desalination cell (PMDC) technologies which efficiently remove salts from saline water while providing a dual benefits of simultaneous wastewater treatment and power generation [5]. However, the high cost of membranes including anion exchange membranes (AEM) and cation exchange membranes (CEM) which poses a significant hurdle. Membranes are essential in the bioelectrochemical systems (BES) because they facilitate ion transfer from anodic to cathodic chambers. The ideal membrane should have high proton conductivity, low membrane resistance, little oxygen transfer from cathode to anode, a thinner membrane profile, an environmentally benign composition, affordability, resistance to fouling, and fast availability [6]. Synthetic membranes made from a sulfonated polymeric backbone such as Nafion and Ultrex, have good proton conductivity and ion exchange capabilities. However, they have considerable downsides, including high cost, lack of environmental friendliness, increase of MFC internal resistance (R_{int}) substrate crossover from the anode to the cathode chamber, biofouling, pH splitting, undesirable ion crossing, and increased oxygen permeability [7, 8]. The penetration of oxygen to the anode reduces electron flow within the circuit and promotes the growth of aerobic non-electrogenic microorganisms, reducing the efficiency of MFCs [9]. Looking for more cost-effective solutions, researchers are working to identify adequate and affordable separators for MFCs that may be effectively applied. Membraneless-MFCs are increasingly desirable in applications where fouling or cost are major concerns. As a result, several previously reported studies have been conducted to explore alternate materials for these systems. Behera et al. [10] evaluated the performance of MFC with a 4 mm-thick wall made from locally available soil (58–68% kaolinite, 15–26% illite, 5–9% smectite) used as a separator between anode and cathode for proton exchange. Rudra et al. [11] investigated the acid-catalyzed cross-linking of polyvinyl alcohol (PVA) with various glutaraldehyde concentrations for usage in microbial fuel cells. Higher cross-link densities in membranes increased mechanical strength but decreased water uptake and proton conductivity. The 32% cross-linked PVA membrane (PVA3) had the maximum power and current density in MFCs. Overall, the study emphasizes the importance of acid-catalyzed cross-linked PVA membranes in bioenergy conversion using MFCs. Neethu et al. [12] studied the suitability of coconut shell (CS) as a proton exchange membrane (PEM) in MFC and MCC systems. It was found that the discovered that CS had a high-water absorption rate (32%) facilitating proton transport to the cathodic chamber. While CS's proton conductivity was equivalent to Nafion 117, its coefficient of oxygen mass transfer was lower confirming that it performed better as a separator. However, CS demonstrated greater maximum power output and coulombic efficiency (CE) than Nafion 117. Ismail and Radeef [13] studied for the first time the use of discarded PVC wall cover material as a separator to replace the conventional CEM membrane in a microbial fuel cell fueled with potato chips processing wastewater. The suggested membrane-less MFC demonstrated significant results, with COD removal efficiencies of up to 99% with considerable current and power densities of 560.8 mA/m² and 181.1 mW/m², respectively, alongside a low internal resistance of 45 Ω. Das et al. [14] created a low-cost alternative to the Nafion membrane for microbial fuel cells by crosslinking polyvinyl alcohol (PVA) with glutaraldehyde (GA), which addressed difficulties such as biofouling and fuel crossover. The crosslinked PVA membrane has better thermo-mechanical stability, antibacterial characteristics, and a higher power density than traditional membrane for household wastewater treatment. Adam et al. [15] found that the crosslinking polyvinyl alcohol (PVA) membranes with sulfosuccinic acid (SSA) improved proton conductivity resulting in a power density from wastewater, surpassing Nafion membranes. It demonstrated better thermomechanical stability and comparable power density to existing Nafion membranes. The inclusion of zirconium phosphate (ZrP) improved performance even further, demonstrating the PVA/SSA/ZrP membrane's potential as a separator in future MFC applications. Wang et al. [16] created a membrane by combining chitosan (CTS), boron phosphate (BPO_4), and multi-walled carbon nanotubes (MWNTs), resulting in significant improvements in proton conductivity and power density in fuel cell applications. Terbish et al. [17] developed a nano-clay montmorillonite (MMT)/chitosan (Cs) membrane for MFC applications, attaining a power density of 85.7 mW/m² and greatly improving wastewater treatment efficiency compared to neat Cs and Nafion membranes. Palanisamy et al. [18] modified chitosan by introducing sulfonic acid (SO_3H^-) groups to increase its proton conductivity, followed by blending this sulfonated chitosan (sCS) with polyvinylidene fluoride polymer and added functionalized SiO_2 containing OH^- groups. This combination was used to create chitosan-based composite proton exchange membrane (PEM). Chauhan et al. [19] created a proton exchange membrane (PEM) for single-chamber MFC utilizing composites of lithium-doped zinc oxide (ZnO) and polyvinyl alcohol (PVA). The produced Li-doped ZnO was evaluated through physiochemical investigation using FT-IR, XRD, TEM, and AC impedance. Incorporating 2.0% Li into the PVA-ZnO membrane increased power generation in the MFC, demonstrating potential as an efficient and cost-effective separator for MFC applications, with observed improvements in electrochemical behavior and proton conductivity, as well as decreased biofouling. Atkar et al. [20] synthesized blended membranes, SPVA/SCS, via solution-casting and solvent evaporation, optimizing a blend of polyvinyl alcohol (PVA) and chitosan (SCS) based on factors such as film-forming ability, cost-effectiveness, and proton conductivity. Sulfonic groups were incorporated into the polymer chain to enhance proton conductivity. Membranes with varying mass ratios of SPVA/SCS including 90:10, 50:50, and 10:90 successfully synthesized and characterized for their thermal stability and chemical structure. Abdel-Motagali et al. [21] investigated the potential of utilizing a hybrid nanocomposite (HNC) membrane for proton exchange in water electrolysis. The durability of the HNC membrane was significantly improved, extending from just a few hours to several hundred hours, by sandwiching it between two partially coated Nafion 212 membranes.

In spite of the numerous previously reported studies available on membrane-less MFC, yet, none of the previously reported studies have considered and investigated the followings;

(1) membrane-less photosynthesis microbial desalination cell (PMDC) for simultaneous desalination of saline/ brackish water and reclamation of wastewater associated with bioenergy recovery.

(2) the potential of using a polymeric cost-effective material as a separator to replace both the cation exchange membrane and anion exchange membrane in a PMDC.

This study fills up this gap for the first time by exploring a novel application of PE foam self-adhesive wallpaper (PEFSW) as a separator to replace the typical cation and anion exchange membranes in a tubular enclosed PMDC used for simultaneous desalination of real seawater, and treatment of real domestic wastewater associated with bioenergy recovery. This investigation represents a significant step forward in the development of sustainable and integrated solutions for water treatment and energy generation.

2. Materials and methods

2.1. Source and type of wastewater

Samples of real domestic wastewater were collected from a sewage treatment plant located in Baghdad, Iraq. The anodic chambers in the PMDC systems were continually fed with the raw untreated real domestic wastewater in the PMDC systems. Initial concentrations of organic content in the domestic wastewater samples were ranged from 400 to 800 mg COD/L.

2.2. Actual seawater

Real samples of seawater (SW) were grabbed from the inlet pipe to a water treatment and desalination station at Al-Faw district, Al-Basrah city, Iraq. Concentrations of total dissolved solids (TDS) in the raw seawater samples were in the range of 20000 - 45000 mg/L. NaCl-based aqueous solution was prepared of 10000 mg/LTDS initial concentration, and continuously fed into the desalination chamber for 20 days began from the startup of the PMDC systems. Then at day 21 it was replaced by the real seawater to the end of operation period. The reason behind using the

synthetically prepared saline aqueous solution before the real seawater was to restrict or prevent the influence of the fluctuation of TDS concentrations in the real seawater on the potential of initiating the desalination process in the PMDCs.

2.3. Microbial community characterization and microalgae identification

To initiate the growth of the anodic biofilm, the anodic compartment was inoculated with activated sludge samples which were grabbed from a sewage treatment plant in Baghdad, Iraq. The collected samples were instantly transferred to the laboratory and preserved at 4°C to maintain their physicochemical properties. Then after, the samples were centrifuged and cultured using a variety of culture media including McConkey and blood agars. Characterization of the biomass samples was performed according to the procedure reported by Hou et al. [22]. Results demonstrated that the predominant bacterial species in the sludge samples were *Bacillus albus, Bacillus cereus, Bacillus tropicus, Bacillus thuringiensis, Bacillus licheniformis, Bacillus paramycoides, Staphylococcus haemolyticus.* and *Escherichia coli*.

Molecular phylogenetic analysis was applied for identifying the microalgae which was used in the biocathode compartments. *Coelastrella* sp. and *Mariniradius saccharolyticus* were identified as the main microalgae used in the biocathode. Blue-green microalgae type was identified using the 16S rRNA gene, whereby, green microalgae type was identified using nuclear ribosomal DNA's internal transcribed spacers (ITS) to detect sequence variation.

To produce these microalgae, optimal conditions were determined using the methods described by Barahoei et al. [23]. This entailed providing fluorescent lamps to supply the light required for microalgae production. In addition, conventional BG11 media was used to cultivate the microalgae. These changes ensured that the identified microalgae species could grow and thrive in the PMDC system's biocathode compartments.

2.4. PE foam self-adhesive wallpaper

The high cost, in addition to low ion selectivity of the typical membranes types used in the MDC and PMDC systems including cation exchange membrane (CEM) and anion exchange membrane (AEM), impairing not only the energy and coulombic efficiency of the system but also limiting a wide practical application of this potential sustainable technology. Accordingly, it becomes necessary to find and search for efficient and cost-effective alternatives for separating the compartments in these sustainable systems. In this study, a recycled waste material of PE foam self-adhesive wallpaper (PEFSW) was used for the first time to replace the CEM and AEM in the PMDCs systems. It is an eco-friendly material. It is characterized by being a durable, lightweight, resilient, closed-cell material, nontoxic, odorless, waterproof material, soft and anti-collision. The thickness of PEFSW was 2.5 mm and exhibited a porous, hydrophilic structure that enabled ion transport with measured ionic conductivity of ~ 200 mS/cm, tensile strength of 42.84 MPa, and chemical stability at pH range of 1-10. Sample of the PEFSW versus the typical CEM and AEM is shown in Fig. 1.

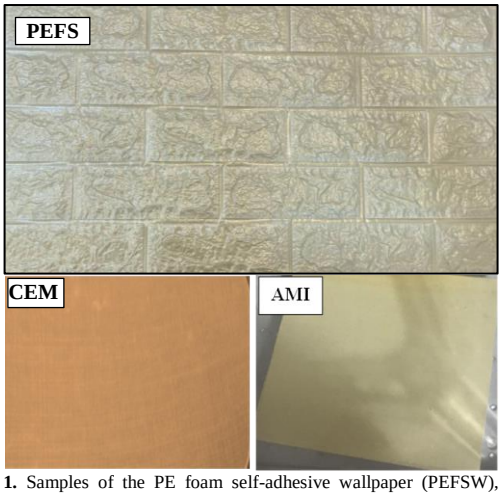

Fig. 1. Samples of the PE foam self-adhesive wallpaper (PEFSW), cation exchange membrane (CEM), anion exchange membrane (AEM).

2.5 Installation and setup of PMFC systems

In this study, two identically designed a three sequential cuboid compartments photosynthesis microbial desalination cells (PMDCs) were constructed, setup, and operated in a continuous mode for six months. Both PMDCs were made of Plexiglas material. Each PMDC consisted of three chambers which were the anodic chamber, desalination (mid) chamber, and cathodic chamber. For the membraneless-PMDC, PE foam self-adhesive wallpaper (PEFSW) was used for separation the three compartments, whereby, the compartments of membrane-PMDC were separated by CEM and AEM. The CMI-7000 cation exchange membrane (CEM) was used in PMDC2 to isolate the cathode and desalination chambers. The AMI-7000 cation exchange membrane (AEM) was used to isolate the anode and desalination chambers. Both of the CEM and AEM were supplied by the Membrane International INC., NJ, USA. The technical properties of the CMI-7000S membrane and AMI-7001S are shown in Table 1. Both types of membranes were soaked in 5% NaCl solution for 12h before use.

Table 1
Technical specification of cation exchange membrane.

Property	CMI-7000S Single Sheet	AMI-7001S Single Sheet
Functionality	Strong acid cation exchange membrane	Strong base anion exchange membrane
Polymer structure	Gel polystyrene cross lied with divinylbenzene	Gel polystyrene cross linked with divinylbenzene
Functional group	Sulphonic Acid	Quaternary ammonium
Ionic for	Sodium	Chloride
Color	Brown	Pale yellow
Standard size	1.22m x 3.05m	1.22m x 3.05m
Standard thickness	0.45 ± 0.025 (mm)	0.45 ± 0.025 mm
Electrical resistance	< 30 (Ohm.cm^2)	< 40 (Ohm.cm^2)
Maximum current density	< 500 (Amp/m^2)	< 500 (Amp/m^2)
Permselectivity	94 %	90 %
Total exchange capacity	1.6 ± 0.1 (meq/g)	1.3 ± 0.1 (meq/g)
Water permeability	< 3 (ml/h/ft^2)	< 3 (ml/h/ft^2)
Mullen burst test strength	> 80 psi	> 80 (psi)
Thermal stability	90°C	90°C
Chemical stability	pH range (1-10)	pH range (1-10)

Each of the anaerobic bioanode and aerobic biocathode chambers contained two plain graphite electrodes. The dimensions of each electrode were 2cm×8cm×0.4cm for width, height, and thickness, respectively. Dimensions of the bioanode compartment in each PMDC system were 10cm×25cm×10cm, whereby, for the biocathode and desalination compartments they were 10cm×15cm×10cm for width, length, and height, respectively. Prior to constructing the PMDCs, all the components were properly cleaned with distilled water. For membrane-PMDC, to ensure appropriate proton passage, the AEM and CEM membranes were pre-treated with a 5% NaCl solution for 12 hours before being washed with deionized water. The PMDCs were simultaneously and continuously fed with actual wastewater at a flow rate of 1.04 ml/min via a variable-speed peristaltic pump (Type: BT100S, GOLANDER PUMP, USA) The hydraulic retention time (HRT) in each PMDC systems was set at 36h. Fig. 2 depicts the schematic diagrams of the PMDCs. For the first 20 days, the desalination chamber received a continuous feed of the synthetically prepared saline solution at a flow rate of 0.5 ml/min, which was then replaced with actual saline seawater. Carbon dioxide produced in the anode compartment was transported to the biocathode compartment through a plastic tube to be utilized by the microalgae via photosynthesis. The sole source for oxygen production in the aerobic biocathode chamber was the microalgae. Therefore, both the growth of microalgae and dissolved oxygen (DO) concentrations were monitored on a daily basis in the biocathode throughout the operation period.

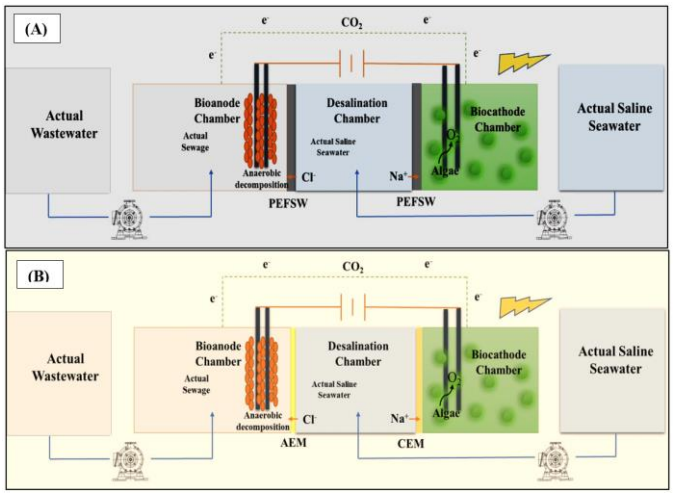

Fig. 2. Schematic diagram of; (A) of membraneless-PMDC, and (B) membrane-PMDC.

2.6. Methods of analysis

Measurements of chemical oxygen demand (COD) concentrations were conducted using a COD analyzer (DR/870 Colorimeter, HACH, USA). DO concentrations were measured using dissolved oxygen meter type YSI 5100. Total dissolved solids (TDS) concentrations were determined following the procedure outlined in the *Standard Methods* [24], with cross-checking using TDS meter (Hanna Instruments).

The growth of microalgae was determined by measuring the optical density (OD) of the microalgae at a wavelength of 620 nm using a Maxwell® RSC instrument (Promega). The concentration of microalgae dry biomass was then calculated using the following formula [25]:

$$\text{Microalgae concentration} = \frac{\text{absorbance at wavelength 620 nm}}{0.8702} \quad (1)$$

Continuous recording of the voltage was carried out by using a data logger and a digital multimeter as well. For the closed circuit, a 120-Ohm resistor was employed. Electrical current (*I*) was calculated using Ohm's law (Eq.2) as follows:

$$I = \frac{V}{R} \quad (2)$$

The power was calculated using the Eq. (3)

$$P = V \times I \quad (3)$$

where; V is the voltage, R is the resistance, and P is the power.

Polarization curves is a potential tool to reflect and analyze the performance of the electrochemical and bioelectrochemical systems. The data necessary for plotting the polarization curve were obtained by using variable external resistors in the range 5-100,000 Ω.

In order to describe the complex interrelated processes occurring in the proposed PMDC system in this study, four kinetic models for biofilm growth were adopted including; Monod, Blackman, Tessier, and Moser models. The models were solved using MATLAB software (version R2021a), in particular the Ode45 solver and Excel solver tools.

3. Kinetics modeling of anodic biofilm growth

Studying the kinetic of biofilm growth is important due to the strong interrelation between the anodic biofilm growth and the complex of bioelectrochemical processes occurs in the PMDC which may affect the performance and fouling of the separators between the different chambers. Several models for bacterial growth kinetic are available to describe the biochemical reactions ranged from low to high concentrations of substrate. These models are normally esteemed by using the determination coefficient (R^2). The value of R^2 is employed to evaluate the effectiveness of a model, and its proximity to 1 indicates a reliable and accurate measure of the model's predictive validity [26]. In this study, the fluctuated substrate concentrations and mixed structure of the anodic biofilm necessitated the examination of the biofilm growth kinetics. Four various models were examined to comprehensively describe the bacterial growth and the related biochemical reactions. These kinetic models are evaluated to assess the most appropriate one for the target case:

1- Monod model; a basic and commonly used formula (Eq.4) to describe bacterial growth in relation to substrate utilization as follows [27]:

$$\mu = \mu_{max} \times \frac{S}{K_S + S} \quad (4)$$

2- Blackman model, which is formulated by Eq.5 [27]:

$$\mu = \mu_{max} \times \frac{S}{2K_S} \quad (5)$$

3- Tessier model, which is formulated by Eq.6 [28]:

$$\mu = \mu_{max} \times \left(1 - e^{-\frac{S}{K_S}}\right) \quad (6)$$

4- Moser model, formulated by Eq. 7 [29]:

$$\mu = \mu_{max} \frac{S^n}{K_s + S^n} \quad (7)$$

where; "μ" is the specific growth rate (h^{-1}), μ_{max} is the maximum specific growth rate (h^{-1}) k_s is a proportional constant (mg/L), S is the substrate concentration (mg/L). The Moser model with its "n" parameter is a factor that can be easily adjusted so that it will suit the experimental data contrary to the fact that the bioreactor reaction is always dynamic. In microbial fuel cells and microbial desalination cell systems, the substrate biodegradation rate (r) and maximum substrate biodegradation rate (r_{max}) are frequently substituted with the specific growth rate and maximum specific growth rate, respectively. The rates are primarily determined by units $kg/m^3.d$, however, the alternate way to express them would be in power or power density units, in which power is usually represented as mW or mW/m^3 in the case of power density, accordingly [30].

4. Results and discussion

4.1 Performance of membraneless-PMDC versus membrane-PMDC

Performance of the suggested PMDC systems was evaluated in terms of organic content removal efficiency, desalination efficiency, and power generation. The profiles and trends of the organic content removal efficiency from the actual domestic wastewater in the anode compartments of the PMDCs are presented in Fig. 3. It is obvious that the profiles consist of two phases; fast rate removal of COD in the first phase which lasted for 10 days followed by achieving a steady state conditions and stable removal rate during the second phase. A significant comparable efficiencies of organic content removal were clearly observed in membraneless-PMDC and membrane-PMDC with maximum COD removal efficiencies of 99.6% and 98.1%, respectively. This remarkable removal of organic matter was obtained within a short timeframe of only 10 days, indicated that the substrate provided a favorable environment for the proliferation of biofilm bacterial species. Moreover, the significant high efficiency of the organic content removal and its high stability observed in the membraneless-PMDC revealed a superior performance of the novel use of PEFSW as a separator between the PMDC chambers to replace both the CEM and AEM, indicating its capability to function as CEM and AEM as well. The obtained results of COD removal efficiency indicated the competitive and superior performance of PEFSW makes it a potential innovative option versus the typical CEM and AEM normally used in the conventional membrane-PMDC fueled with different types of substrates as outlined in the previously reported studies. Nadzri et al. [31] suggested 49% and 53 % COD reduction from synthetically prepared wastewater using alternatively *Chlamydomonas* sp. (UKM6) and *Scenedesmus* sp. (UKM9) in a cylindrical-shaped membrane -PMDC with microalgae cathode. Bejjanki et al. [32] reported a COD elimination efficiency of 80.2 ± 0.5% from dairy wastewater using *Oscillatoria* sp. as the biocatalyst in a membrane-PMDC. Results obtained by Danaee et al. [33] revealed a 50% removal efficiency of COD from a mixture of human feces and urine in a membrane-PMDC. Sadeq and Ismail [34] suggested 99.3% removal efficiency of organic content from actual domestic wastewater in a tubular membrane-PMDC inoculated with mixed bacterial species. Sadeq and Ismail [35] reported a 99% removal efficiency of COD from real sewage in enclosed cuboid compartments membrane-PMDC inoculated with mixed bacterial species.

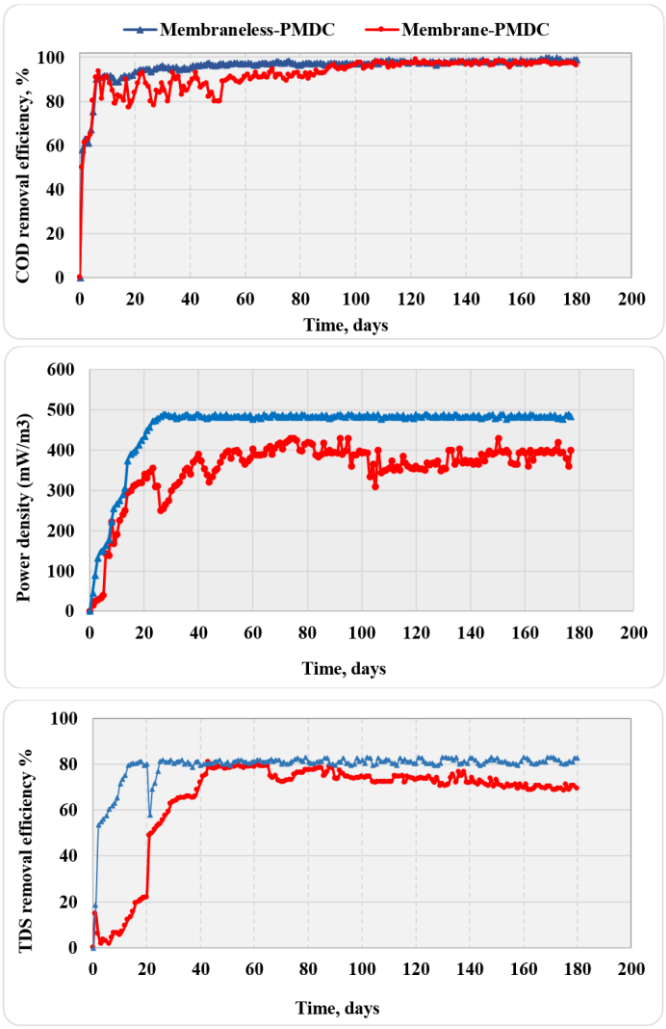

Fig.3. The performance of membraneless-PMDC versus membrane-PMDC in terms of COD removal efficiency, power recovery, and desalination efficiency.

For energy recovery, the results demonstrated maximum power output of 489 mW/m³ and 430 mW/m³ the in the membraneless-PMDC and membrane-PMDC, respectively. However, a high stability of power output in the membraneless-PMDC was observed compared to the notable fluctuation power in the membrane-PMDC indicating the potential of PEFSW performance. On the other hand, the results of desalination efficiency were quite interesting. As shown in Fig. 3, the profiles of desalination efficiency consist of two remarkable phases for both PMDCs. During the first 20 days of operation, the PMDCs run with synthetically prepared NaCl-based saline solution. It is obvious that the desalination process started from the first day and sharply increased until day 13, then a kind of stability was observed and lasted for 2 days before introducing the real seawater into the desalination chamber. Then immediately after replacement of the saline solution by the real seawater at day 20, an instantaneous drop in the desalination efficiency was noted, followed by a rerise of the desalination efficiency which continued at a very stable manner in the membraneless-PMDC and with relatively less stability throughout the entire period of operation in spite of the salinity fluctuation in the real seawater. Maximum desalination efficiencies observed in the membraneless-PMDC and membrane-PMDC were 83% and 81%, respectively, another proof for the significant validity of the novel use of PEFSW as a separator between the membraneless-PMDC chambers. Compared to membrane-PMDC. Although the desalination efficiencies in the PMDCs were relatively comparable, however, the profile of TDS removal in the membraneless-PMDC exhibited more stability compared to membrane-PMDC.

The stability in power generation and TDS removal efficiency in the membraneless-PMDC may be attributed to several material properties inherent to Pe self-adhesive wallpaper (PEFSW) that differ from the traditional membranes. The improved ionic transport observed with (PEFSW) might be due to the fact that wall adhesives materials often contain polymers such as polyvinyl alcohol (PVA) and polyethylene glycol (PEG) characterized by high ionic conductivity [36]. To support this, the adhesives can also adopt a porous structure having interconnected pathways, making it easier for ions to move through them compared to the dense nature of traditional membranes. The other outstanding factor is the reduced or absence of biofouling because they could have surface features preventing microbial colonization that optimize ion mobility as well as whole cell performance [37]. They can also be tailored in order to incorporate stronger affinity for certain ions hence enhancing separation and transportation procedures. This way, they create an ideal environment for ionic movement resulting into great performance improvement in microbial desalination cells at large scale [38].

In conclusion, although the experimental findings showed that the COD removal and desalination efficiencies in both the membraneless PMDC and membrane PMDC were relatively comparable, however, the membraneless-PMDC exhibited a slightly higher efficiencies associated with faster achievement of steady state conditions compared to membrane-PMDC. Also, the observable difference in power generations between the two PMDCs. Moreover, the most interesting observation in this study was the absence of PEFSW fouling during the operation period. Also, using a single type of separator in the PMDC instead of two different types of membranes is a bonus. According to these significant observations, the membraneless-PMDC can effectively compete with membrane-PMDC, indicating that the PE foam self-adhesive wallpaper (PEFSW) is a powerful cost-effective option to replace the costly typical cation and anion membranes.

4.2. Microalgae growth and oxygen production in the PMDC systems

The profiles of the microalgae concentration and DO concentrations in the biocathode compartments of membraneless-PMDC and membrane-PMDC are presented in Fig. 4. The presented data exhibits three clearly distinguishable phases that correspond to the microalgae growth and DO concentration during the entire operation. The first phase, was characterized by the slow microalgae growth during the first 10 days of operation suggesting that the initial establishment of the microbial community and microalgae growth was gradual. The slow growth may be attributed to the acclimation period required for microorganisms to adapt to the new environment and conditions within the PMDC systems. However, the concentration of DO increase in a fast manner during the first 10 days of operation. Then after, the DO concentration gradually increased until day 120 of continuous operation. This observation could be attributed to the fact that initially there was a certain DO concentration available in the catholyte, but after a while this oxygen was consumed as a reductant which is essential as a reductant for sustained power production. Hence, after 10 days the microalgae were the only source for the available DO. This phase highlights the importance of monitoring and adjusting the operational parameters during the early stages to support microbial growth and ensure sufficient oxygen supply. For phase 2, it started from the day 11until the end of day 120 of continuous operation. This phase exhibited an observable increase in both microalgae concentration and DO levels. The rise in microalgae concentration may be attributed to improved nutrient availability, optimized growth conditions, or reduced competition among microorganisms. The stable increase in DO concentration indicated that the system maintained sufficient oxygen levels, which is crucial for facilitating the biological processes involved in power generation. This phase demonstrated the potential for optimizing the PMDC systems to support increased microalgae growth and power generation, contributing to improved overall efficiency. Phase 3 exhibited a high growth rate in microalgae concentration while maintaining stable and sufficient DO levels. This phase signified the establishment of a well-balanced and sustainable microbial community within the PMDC systems. The high microalgae growth suggested the successful adaptation and proliferation of microorganisms in the biocathode compartments, leading to enhanced power production. The consistent DO concentration throughout Phase 3 further confirmed the system's ability to maintain a favorable environment for efficient microbial activity. This phase highlights the potential for long-term stable operation and sustained power generation in the PMDC system, provided that appropriate conditions and maintenance practices are upheld. In conclusion, the observation of distinct phases in the PMDC systems sheds light on the dynamic interactions between microalgae growth and DO concentration, both crucial factors for power generation. Understanding these growth dynamics and their correlation with power production is essential for optimizing the PMDC operation and maximizing power generation efficiency. The findings from this study contribute valuable insights into the design and management of PMDC systems, facilitating their application as sustainable and eco-friendly power generation technologies with the potential for broader implementation in the future.

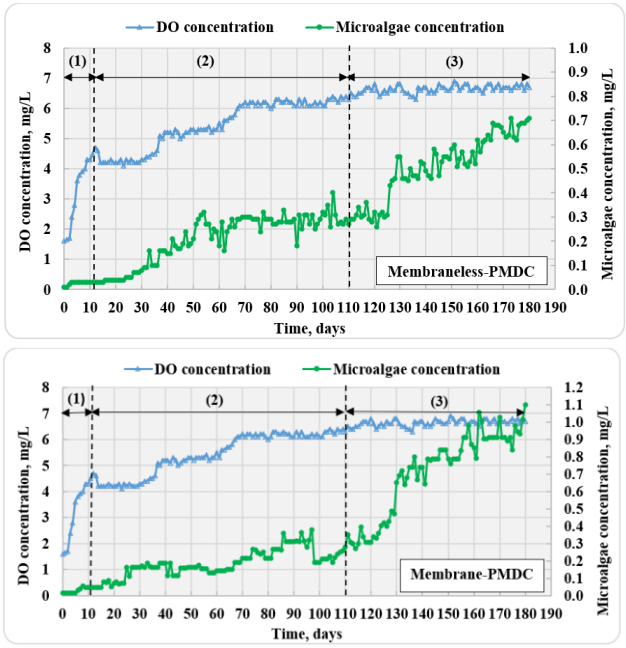

Fig. 4. Profiles of dissolved oxygen (DO) and microalgae concentrations in the cathodic compartment.

4.3. Polarization study

Polarization curves play a crucial role in characterizing the performance of PMDC systems. Polarization curves are an effective method for describing and analyzing the performance of PMDC systems. Maximum available current and power were generated when the external and internal resistances were equal. Fig. 5 illustrates the relation between the voltage and power output as a function of the current for the membraneless-PMDC and membrane-PMDC. Both membraneless-PMDC and membrane-PMDC exhibited noteworthy performance. For the membraneless-PMDC, at an internal resistance of 90 Ω, a maximum power density of 29.9 mW/m^2 and a current density of 157.5 mA/m^2 were achieved. For membrane-PMDC, maximum power and current densities were 35.7 mW/m^2 and 133.3 mA/m^2, respectively at internal resistance of 150 Ω suggesting a specific operating point that maximized energy conversion. These results indicated the ability of the system to efficiently convert available energy into electrical power. Also, the results revealed that the both PMDCs yielded distinct optimal conditions for power and current density. The membraneless-PMDC system exhibited its best performance at an internal resistance of 90 Ω, while the membrane-PMDC system achieved its peak values at 150 Ω internal resistance.

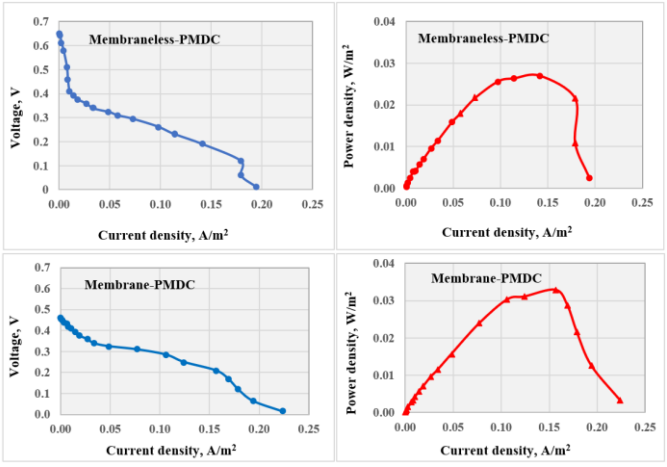

Fig. 5. Polarization curves represented by power density versus current density, and voltage versus current density in the membraneless-PMDC and membrane-PMDC.

4.4. Coulombic efficiency (CE)

The CE values under steady-state conditions were calculated using the following formula [39]:

$$\text{Columbic efficiency } (CE) = \frac{MI}{F.bq.\Delta COD} \quad (8)$$

Maximum daily and optimum steady-state CE values for the PMDCs in each day and steady-state conditions are presented in Fig. 6.

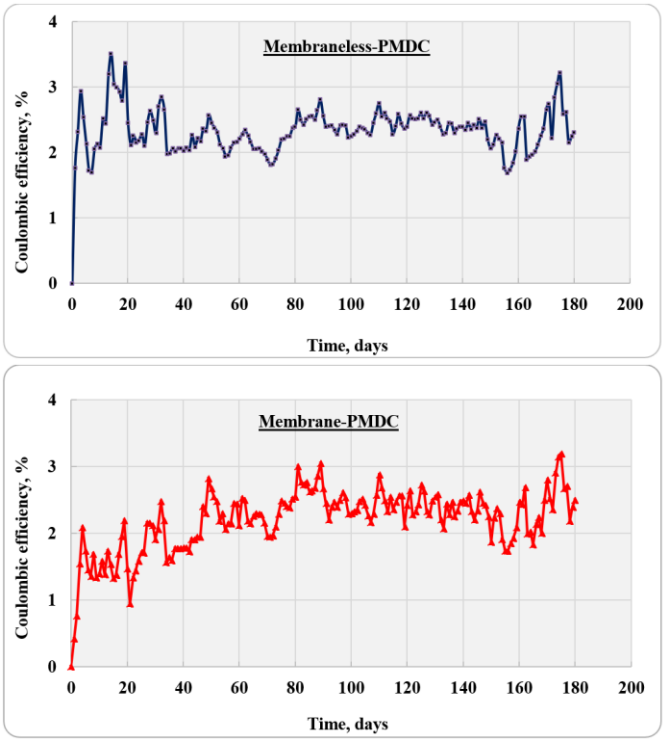

Fig. 6. Profiles of the coulombic efficiency in the membraneless-PMDC and membrane-PMDC.

Maximum CE values achieved during the operational period in the membraneless-PMDC and membrane-PMDC were 3.51%. and 3.46%, respectively. These results could be considered superior compared to the 0.04% reported by Park et al. [40] for the treatment of starch-processing wastewater. It is important to mention that the CE is not a kinetic parameter and is therefore not directly related to power densities. Low CE values can be attributed to the low densities of anode-respiring microorganisms in the anodic biofilm, which can be caused by competition for space between bacteria. This, in turn, can contribute to the reduction of power density as suggested by [41]. In addition, it is known that the CE is inversely proportional to COD removal and substrate flow rate. Several studies have reported that the consumption of organic substrates by non-electrogenic bacteria can lead to the diversion of electron movement toward alternative metabolic processes, potentially resulting in lower CE values despite higher COD removal efficiency [42-44]. These non-electrogenic counterparts have the ability to consume organic substrates, thus diverting the electron flux away from electricity generation and leading to a decrease in CE values. This diversion towards alternate metabolic pathways, although contributing to COD removal efficiency, can counterintuitively yield lower CE values due to the reduced portion of electrons contributing to current generation. These intricacies find support in various studies, such as those by Liu et al. [42] collectively emphasizing the need to consider the interplay of microbial interactions, substrate utilization, and electron flow when interpreting and optimizing CE values [42]. This nuanced perspective underscores the importance of a holistic approach in the assessment and advancement of microbial electrochemical systems, providing insights into the delicate balance between various factors that shape their performance characteristics.

4.5. Kinetic models

As previously reported in section 3, Monod, Blackman, Teissier, and Moser kinetic models were individually employed to predict the power generated over time as a function of the substrate utilization, which implicitly reflected the growth of biofilm. The graphical presentation of the predicted results is depicted in Fig. 7. For the membraneless-PMDC, the results indicated that the Blackman model showed excellent consistency with the experimental growth data, achieving a determination coefficient (R^2) of 0.95. Furthermore, the Monod, Teissier, and Moser models also exhibited excellent

agreement with the experimental data, revealing R^2 values of 0.94, which suggests that the reaction rates are dependent on a non-inhibitory substrate and can adequately describe the slow growth of bacteria [45]. These findings suggest that the Blackman model is the most suitable for predicting the growth of bacteria in the membraneless-PMDC during system operation. Table 2 illustrates the assessed kinetic parameters and their validation.

For both PMDC systems, it is well observed that the predicted results by the four examined kinetic models for bacterial growth were relatively comparable and fitted well the experimental data with a determination coefficient (R^2) ranged between 0.94 to 0.96.

5. Conclusion

This study highlights the potential of reusing for the first time the application of self-adhesive PE wallpaper waste material (PEFSW) as a novel separator to replace expensive membranes in photosynthetic microbial desalination cells (PMDCs). The results demonstrated impressive maximum removal efficiencies of salinity and organic content accompanied with maximum power generation in the membraneless-PMDC of 83%, 99.6% and 489 mW/m^3 versus 81%, 98.1%, and 430 mW/m^3, respectively observed in the conventional membrane-PMDC. The study suggested that the use of PE foam waste (PEFSW) could provide an environmentally friendly and cost-effective alternative to expensive cation and anion exchange membranes in bioelectrochemical systems, especially in systems that require both types of membranes simultaneously such as MDC and PMDC. Importantly, PEFSW does not need to be pre-treated before use, unlike conventional membranes which usually require chemical pre-treatment. In addition, this study revealed excellent agreement between experimental and predicted results for both biofilm growth kinetic models and the electrochemical models as well. Future work is proposed to be extended to evaluate the performance of the membraneless-PMDC from lab-scale to pilot plant large-scale. Furtherly, the work will be extended to investigate the potential of other materials to be utilized as separators in the sustainable bioelectrochemical systems for important applications in water treatment and renewable energy generation.

Acknowledgment

The authors gratefully acknowledge the Material Physics Laboratory, Department of Physics, LPPM-Universitas Negeri Surabaya (UNESA), for facilities supporting this work.

Conflicts of Interest

The authors declare that there are no conflicts of interest.

Declaration of competing interest

The authors declare that they have no known competing financial interests or personal relationships that could have appeared to influence the work reported in this paper.

Credit authorship contribution

Z. Z. Ismail: Conceptualization, Data curation, Formal analysis, Project administration, Supervision, Validation, Writing-review and editing.
A. M. Sadeq: Conceptualization, Investigation, Resources, Visualization, Writing-original draft.

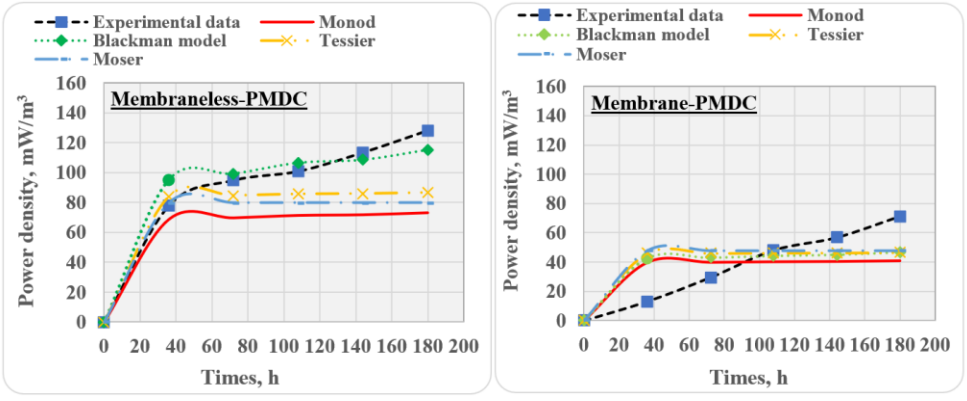

Fig. 7. Kinetic models for the anodic biofilm growth expressed in terms of power generation in the membraneless-PMDC and membrane-PMDC.

Table 2
Kinetic models for the anodic biofilm growth expressed in terms of power generation in the PMDC systems.

Model	Kinetic parameters					
	P_{max}	K_s	R^2	n	m	S_m
	Membraneless-PMDC					
Monod	105	285.3	0.94	-	-	-
Blackman	74.9	185.7	0.95	-	-	-
Tessier	90.0	174.9	0.94	-	-	-
Moser	80.0	190.0	0.94	1.80	-	-
	Membrane-PMDC					
Monod	58.0	240.0	0.95	-	-	-
Blackman	28.0	169.9	0.94	-	-	-
Tessier	48.4	176.0	0.96	-	-	-
Moser	48.0	260.0	0.96	1.80	-	-

References

[1] Y. Xu, R. Quan, J. Zhou, H. Mao, C. Li, S. Ma, J. Mou, H. Zhou, High-capacity and high-stability capacitive desalination with dual redox-active MnCo2S4/g-C3N4 heterojunction electrode. Sep. Purf. Technol. 355 (2025) 129761. https://doi.org/10.1016/j.seppur.2024.129761

[2] S.M. Alawad, R.B. Mansour, F. A. Al-Sulaiman, S. Rehman, Renewable energy systems for water desalination applications: A comprehensive review. Energy Convers. Manag. 286 (2023) 117035. https://doi.org/10.1016/j.enconman.2023.117035

[3] S.M.J.S. Sabour, B. Ghorashi, A comprehensive review of major water desalination techniques and mineral extraction from saline water. Sep. Purf. Technol. 349, 127913. https://doi.org/10.1016/j.seppur.2024.127913

[4] A.C. Sophia, V.M. Bhalambaal, E.C. Lima, M. Thirunavoukkarasu, Microbial desalination cell technology: contribution to sustainable waste water treatment process, current status and future applications. J. Environ. Chem. Eng. 4 (2016) 3468-3478. https://doi.org/10.1016/j.jece.2016.07.024

[5] X. Cao, X. Huang, P. Liang, K. Xiao, Y. Zhou, X. Zhang, B.E. Logan, A new method for water desalination using microbial desalination cells. Environ. Sci. Technol. 43 (2009) 7148-7152. https://doi.org/10.1021/es901950j

[6] A. Banerjee, R.K. Calay, F.E. Eregno, Role and important properties of a membrane with its recent advancement in a microbial fuel cell. Energies 15 (2022) 444. https://doi.org/10.3390/en15020444

[7] M.J. González-Pabón, F. Figueredo, D.C. Martinez-Casillas, E. Corton, Characterization of a new composite membrane for point of need paper-based micro-scale microbial fuel cell analytical devices. PLoS One 14 (2019) e0222538. https://doi.org/10.1371/journal.pone.0222538.

[8] J. Ramirez-Nava, M. Martínez-Castrejón, R.L. García-Mesino, J.A. López-Díaz, O. Talavera-Mendoza, A. Sarmiento-Villagrana, F. Rojano, G. Hernández-Flores, The implications of membranes used as separators in microbial fuel cells. Membranes 11 (2021) 738, 1-27. https://doi.org/10.3390/membranes11100738.

[9] C. Prestigiacomo, C.M. Fernandez-Marchante, F.J. Fernández-Morales, P. Cañizares, O. Scialdone, M.A. Rodrigo, New prototypes for the isolation of the anodic chambers in microbial fuel cells. Fuel 181 (2016) 704-710. https://doi.org/10.1016/j.fuel.2016.04.122.

[10] M. Behera, P.S. Jana, M.M. Ghangrekar, Performance evaluation of low-cost microbial fuel cell fabricated using earthen pot with biotic and abiotic cathode. Bioresour. Technol. 101 (2010) 1183-1189. https://doi.org/10.1016/j.biortech.2009.07.089.

[11] R. Rudra, V. Kumar, P.P. Kundu, Acid catalysed cross-linking of poly vinyl alcohol (PVA) by glutaraldehyde: effect of crosslink density on the characteristics of PVA membranes used in single chambered microbial fuel cells. RSC Adv. 5 (2015) 83436-83447. https://doi.org/10.1039/C5RA16068E.

[12] B. Neethu, G.D. Bhowmick, M.M. Ghangrekar, Enhancement of bioelectricity generation and algal productivity in microbial carbon-capture cell using low-cost coconut shell as membrane separator. Biochem. Eng. J. 133 (2018) 205-213. https://doi.org/10.1016/j.bej.2018.02.014.

[13] Z.Z. Ismail, A.Y. Radeef, A novel application of polyvinyl chloride (PVC) waste material to Replace membrane in microbial fuel cell treating actual potato chips processing wastewater. J. Systematics, Cybernetics, and Informatics (JSCI) 17 (2019)82-87.

[14] B. Das, S.S. Gaur, A.R. Katha, C.T. Wang, V. Katiyar, Crosslinked poly (vinyl alcohol) membrane as separator for domestic wastewater fed dual chambered microbial fuel cells. Int. J. Hydrogen Energy 46 (2021) 7073-7086. https://doi.org/10.1016/j.ijhydene.2020.11.213.

[15] M.R. Adam, A.A.M. Hassan, M.H.D. Othman, M.H. Puteh, A.F. Ismail, M.A. Rahman, J. Jaafar, Fabrication and characterization of hybrid poly (vinyl alcohol) based proton exchange membrane for energy generation from wastewater in microbial fuel cell system. Int. J. Energy Res. 46 (2022) 23418-23432. https://doi.org/10.1002/er.8639.

[16] J. Wang, T. Qu, J. Ni, F. Cheng, F. Hu, Y. Ou, C. Gong, S. Wen, X. Chen, H. Liu, Composite proton exchange membranes based on inorganic proton conductor boron phosphate functionalized multi-walled carbon nanotubes and chitosan. Surfaces Interfaces 36 (2023) 102557. https://doi.org/10.1016/j.surfin.2022.102557.

[17] N. Terbish, S.R. Popuri, C.H. Lee, Improved performance of organic–inorganic nanocomposite membrane for bioelectricity generation and wastewater treatment in microbial fuel cells. Fuel 332 (2023) 126167. https://doi.org/10.1016/j.fuel.2022.126167.

[18] G. Palanisamy, A.P. Muhammed, S. Thangarasu, T.H. Oh, Investigating the sulfonated chitosan/polyvinylidene fluoride-based proton exchange membrane with fSiO2 as filler in microbial fuel cells. Membranes 13 (2023) 758, 1-19. https://doi.org/10.3390/membranes13090758.

[19] S. Chauhan, A. Kumar, S. Pandit, A. Vempaty, M. Kumar, B.S. Thapa, N. Rai, S.G. Peera, Investigating the performance of a zinc oxide impregnated polyvinyl alcohol-based low-cost cation exchange membrane in microbial fuel cells. Membranes 13 (2023) 55. https://doi.org/10.3390/membranes13010055.

[20] A. Atkar, S. Sridhar, S. Deshmukh, A. Dinker, K. Kishor, G. Bajad, Synthesis and characterization of sulfonated chitosan (SCS)/sulfonated polyvinyl alcohol (SPVA) blend membrane for microbial fuel cell application. Mater. Sci. Eng. B 299 (2024) 116942. https://doi.org/10.1016/j.mseb.2023.116942.

[21] A. Abdel-Motagali, S. Al Bacha, W.M.A. El Rouby, J. Bigarré, P. Millet, Evaluating the performance of hybrid proton exchange membrane for PEM water electrolysis. Int. J. Hydrog. Energy 49 (2024) 87-102. https://doi.org/10.1016/j.ijhydene.2023.06.330.

[22] Q. Hou, X. Bai, W. Li, X. Gao, F. Zhang, Z. Sun, H. Zhang, Design of primers for evaluation of lactic acid bacteria populations in complex biological samples. Front. Microbiol. 9 (2018) 2045. https://doi.org/10.3389/fmicb.2018.02045.

[23] M. Barahoei, M.S. Hatamipour, M. Khosravi, S. Afsharzadeh, S.E. Feghhipour, Salinity reduction of brackish water using a chemical photosynthesis desalination cell. Sci. Total Environ. 779 (2021) 146473. https://doi.org/10.1016/j.scitotenv.2021.146473.

[24] American Public Health Association (APHA), Standard methods for the examination of water and wastewater. Washington, DC, USA (2005).

[25] T.J. Arana, V.G. Gude, A microbial desalination process with microalgae biocathode using sodium bicarbonate as an inorganic carbon source. Int. Biodeterior. Biodegrad. 130 (2018) 91–97. https://doi.org/10.1016/j.ibiod.2018.04.003.

[26] S.M.T. Gharibzahedi, S.H. Razavi, M. Mousavi, Kinetic analysis and mathematical modeling of cell growth and canthaxanthin biosynthesis by Dietzia natronolimnaea HS-1 on waste molasses hydrolysate. RSC Chem. 3 (2013) 23495-23502. https://doi.org/10.1039/C3RA44663H.

[27] M.P. Zacharof, R.W. Lovitt, Modelling and simulation of cell growth dynamics, substrate consumption, and lactic acid production kinetics of Lactococcus lactis. Biotechnol. Bioprocess Eng. 18 (2013) 52-64. https://doi.org/10.1007/s12257-012-0477-4.

[28] T. Jafary, A.A. Ghoreyshi, G.D. Najafpour, S. Fatemi, M. Rahimnejad, Investigation on performance of microbial fuel cells based on carbon sources and kinetic models. Int. J. Energy Res. 37 (2013) 1539-1549. https://doi.org/10.1002/er.2994.

[29] M. Muloiwa, S. Nyende-Byakika, M. Dinka, Comparison of unstructured kinetic bacterial growth models. S. Afr. J. Chem. Eng. 33 (2020) 141-150. https://doi.org/10.1016/j.sajce.2020.07.006.

[30] Z.I. Abubakari, M. Mensah, R. Buamah, R.C. Abaidoo, Assessment of the electricity generation, desalination and wastewater treatment capacity of a plant microbial desalination cell (PMDC). Int. J. Energy Water Res. 3 (2019) 213–218. https://doi.org/10.1007/s42108-019-00030-y.

[31] N.A.A. Nadzri, N.H.M. Yasin, M.H. Abu Bakar, S. Thanakodi, M.N.I. Salehmin, M. S. Takriff, M.F. N. Aznan, T. Maeda, Photosynthetic microbial desalination cell (PhMDC) using Chlamydomonas sp. (UKM6) and Scenedesmus sp. (UKM9) as biocatalysts for electricity production and water treatment. Int. J. Hydrog. Energy. 48 (2023) 11860-11873. https://doi.org/10.1016/j.ijhydene.2023.01.142.

[32] D. Bejjanki, K. Muthukumar, T.K. Radhakrishnan, A. Alagarsamy, A. Pugazhendhi, S.N. Mohamed, Simultaneous bioelectricity generation and water desalination using Oscillatoria sp. as biocatalyst in photosynthetic microbial desalination cell. Sci. Total Environ. 754 (2021) 14221. https://doi.org/10.1016/j.scitotenv.2020.142215.

[33] S. Danaee, H. Naghoosi, N.B. Varzaghani, P.H.N. Vo, Biodegradation of human fecal sludge for photosynthetic bioelectricity generation and seawater desalination in a microbial desalination cell. Environ. Technol. 15 (2023) 1-13. https://doi.org/10.1080/09593330.2023.2283406.

[34] A.M. Sadeq, Z.Z. Ismail, Sustainable application of tubular photosynthesis microbial desalination cell for simultaneous desalination of seawater for potable water supply associated with sewage treatment and energy recovery. Sci. Total Environ. 875 (2023) 162630. https://doi.org/10.1016/j.scitotenv.2023.162630.

[35] A.M. Sadeq, Z.Z. Ismail, Improved bioenergy recovery and desalination efficiency using innovative configuration of an upflow triple enclosed cuboid compartments -photosynthesis microbial desalination cell: Experimental and modeling study. Renewable Energy 231 (2024) 121010. https://doi.org/10.1016/j.renene.2024.121010.

[36] M. Ulbricht, Advanced functional polymer membranes. Polymer, 47 (2006) 2217-2262. https://doi.org/10.1016/j.polymer.2006.01.084.

[37] C.M. Kirschner, A.B. Brennan, Bio-inspired antifouling strategies. Annu. Rev. Mater. Res. 42 (2012) 211-229. https://doi.org/10.1039/D4CC05149A.
[38] V. Freger, Nanoscale heterogeneity of polyamide membranes formed by interfacial polymerization. Langmuir 19 (2003) 4791-4797. https://doi.org/10.1021/la020920q.
[39] B.E. Logan, Microbial fuel cells. John Wiley & Sons (2008).
[40] H.S. Park, B.H. Kim, H.S. Kim, H.J. Kim, G.T. Kim, M. Kim, I.S. Chang, Y.K. Park, H.I. Chang, A novel electrochemically active and Fe(III) reducing bacterium phylogenetically related to Clostridium butyricum isolated from a microbial fuel cell. Anaerobe 7 (2001) 297-306. https://doi.org/10.1006/anae.2001.0399.
[41] H.S. Lee, P. Parameswaran, A. Kato-Marcus, C.I. Torres, B.E. Rittmann, Evaluation of energy-conversion efficiencies in microbial fuel cells (MFCs) utilizing fermentable and non-fermentable substrates. Water Res. 42 (2008) 1501-1510. https://doi.org/10.1016/j.watres.2007.10.036.
[42] H. Liu, S.A. Cheng, B.E. Logan, Production of electricity from acetate or butyrate using a single chamber microbial fuel cell. Environ. Sci. Technol. 39 (2005) 658-662. https://doi.org/10.1021/es048927c.
[43] R. Rozendal, H. Hamelers, K. Rabaey, J. Keller, G. Buisman, Towards practical implementation of bioelectrochemical wastewater treatment. Trends Biotechnol. 26 (2008) 450-459. https://doi.org/10.1016/j.tibtech.2008.04.008
[44] S. Strycharz, A. Malanoski, S. Snider, H. Yi, D. Lovley, L. Tender, On the electrical conductivity of microbial nanowires and biofilms. Energy Environ. Sci. 4 (2011) 896-913. https://doi.org/10.1039/C1EE01753E.
[45] S. Kwon, I.K. Yoo, W.G. Lee, H.N. Chang, Y.K. Chang, High-rate continuous production of lactic acid by Lactobacillus rhamnosus in a two-stage membrane cell-recycle bioreactor. Biotechnol. Bioeng. 73 (2001) 25-34. https://doi.org/10.1002/1097-0290(20010405)73:1%3C25::aid-bit1033%3E3.0.co;2-n.